INNOVATIVE MULTI PCNN BASED NETWORK FOR GREEN AREA MONITORING - IDENTIFICATION AND DESCRIPTION OF NEARLY INDISTINGUISHABLE AREAS - IN HYPERSPECTRAL SATELLITE IMAGES

Serban-Vasile Carata[1*], *Mihai-Gabriel Constantin*[2], *Veta Ghenescu*[1], *Mihai Chindea*[3], *Marian Ghenescu*[1]

(1) Institute of Space Science, (2) University Politehnica of Bucharest, (3) UTI Grup
(*) serban.carata@spacescience.ro

ABSTRACT

The paper presents an original neural network approach for region of interest detection and classification in multi-spectral satellite images. The proposed method uses a sequence of Pulse Coupled Neural Networks that identifies plausible regions of interest. These regions are passed to a dimension reduction algorithm, Principle Component Analysis, in order to generate the input data for a Support Vector Machine classifier, that validates the data. The algorithm's parameters are optimized using a Genetic Algorithm. The algorithm is designed to distinguish regions that are extremely similar, such as parks in a city that has entire districts made up of houses with yards. The algorithm has been tested on images provided by the Sentinel-2 satellite, and it proved that it can recall 76.85% of the pixels marked as park in the ground truth data, which was obtained from Open Street Map .

Index Terms— Pulse Coupled Neural Network (PCNN), Principle Component Analysis (PCA), Support Vector Machine (SVM), Genetic Algorithm (GA)

1. INTRODUCTION

Traditionally, only a small number of automated studies have been performed on earth observation imagery (natural disaster evaluation, change detection[1]), mainly because the information is extremely dense and hard to automatically evaluate. On top of this, urban areas present a diverse array of features, such as neighbourhoods with houses, apartment buildings and parks, that might be very similar and close to each other. This paper presents a novel approach for automatic identification of city areas covered by parks, as this information is hard to determine for most world cities, given that green cadastre is an emergent concept in most slightly developed countries. In order to evaluate the quality of life, we find this measurement important.

Satellite images have been used in urban information processing, covering domains including urban change detection [2], land use [3]. Several vegetation indexes have been created [4, 5] as methods of crops and general vegetation surface area assessment, however unlike our approach no learning algorithms were implemented, thus no classification between normal vegetation (grass, gardens) and organized urban parks can be achieved with these approaches.

Pulse Coupled Neural Networks (PCNN), a biologically inspired type of neural network whose design tries to mimic the visual cortex of mammals [6, 7], were used in satellite image change detection applied to wildfire affected areas [8] this paper concluding the usefulness of PCNN in the analysis of satellite images, also pointing out the good segmentation performance achieved by this network over reference segmentation methods [9]. The same performances were also achieved by [1] in a paper that studies the monitoring of power lines from satellite images.

2. PROPOSED METHOD

In this section we will present all the subcomponents of the proposed algorithm, and in the final subsection we will present how these components work together to predict the pixels of an image that represent a park.

2.1. Pulse Coupled Neural Network (PCNN)

2.1.1. Standard PCNN algorithm

The PCNN network is described by the following equations:

$$F_{ij}[n] = e^{-\alpha_F} F_{ij}[n-1] + V_F \sum_k \sum_l M_{ijkl} Y_{kl}[n-1] + S_{ij} \quad (1)$$

$$L_{ij}[n] = e^{-\alpha_L} L_{ij}[n-1] + V_L \sum_k \sum_l W_{ijkl} Y_{kl}[n-1] \quad (2)$$

$$U_{ij}[n] = F_{ij}[n](1 + \beta L_{ij}[n]) \quad (3)$$

$$E_{ij}[n] = E_{ij}[n-1] e^{-\alpha_E} + V_E Y_{ij}[n-1] \quad (4)$$

$$Y_{ij}[n] = \begin{cases} 1 \text{ if } \mathrm{U}_{ij}[n] > E_{ij}[n] \\ 0 \text{ else} \end{cases} \quad (5)$$

where α_F, α_L, and α_E are the time constants; V_F, V_L and V_E are the magnitude adjustments; β is the linking strength of the PCNN. Each neuron is denoted by indices (i, j), and one of its neighboring neurons is denoted with indices (k, l). Feeding component $F_{ij}[n]$ is combined with linking component $L_{ij}[n]$ into neurons internal activity $U_{ij}[n]$. The neuron receives input signals via feeding synapse M_{ijkl} and S_{ij}, the pixel value, and each neuron is connected to its neighbors such that the output signal of a neuron modulates the activity of its neighbors via linking synapse W_{ijkl}. The pulse is able to feed back to modulate the threshold $E_{ij}[n]$ via a leaky integrator, raising the threshold by magnitude V_E, that decreases with time constant α_E. During iterations, when a neurons internal activity $U_{ij}[n]$ exceeds its dynamic threshold $U_{ij}[n]$, a pulse is generated (firings).

2.1.2. Non Binary PCNN algorithm

Even though the binarization step is an essential step in the PCNN algorithm, for our purposes we determined that if the final binarization step is omitted, the resulting image provides helpful fuzzy information. By omitting this last step, at the last iteration of the PCNN algorithm, and returning the U matrix, from equation 4, the algorithm returns a non-binary matrix. This matrix enhances some features while diminishing others. Optimizing the internal parameters of the PCNN algorithm we can control what features are enhanced.

2.2. Principal Component Analysis (PCA)

We have used a PCA [10] algorithm to reduce the dimension of the data from a (q*q*3)-dimensional space to a smaller dimension space, which is determined in the GA optimization stage. Also q, which is the size of the sliding window, is determined in the GA optimization stage.

2.3. Support Vector Machine (SVM)

The SVM [11] algorithm is based on a decision hyper plane, which is basically a border between the classes. In the literature it is clearly shown how the SVM kernels can remap the original data points into a higher space so that they become separable. The classification is considered only for the two class case. In this paper, we strive to separate two classes (park and non park) using a function induced by the examples we have available (training set). The aim is to obtain a classification rule that works well on examples yet unknown (generalization).

2.4. Genetic algorithms (GA)

We have used a genetic algorithm (GA) [12] to optimize the 166 parameters of the PCNN model: the number of iterations n; the linking strength β; the link arrange representing the size of the matrices M/W; the values of the M/W matrix; the time constants $\alpha_F = \alpha_L$ and α_E; the magnitude adjustments $V_F = V_L$ and V_E; besides this the GA optimized the threshold levels of the final algorithm, the principal component analysis parameters and the sliding window size and step. The GA parameters are: chromosome population; crossover rate; mutation rate; elite count; stop generation. The fitness function for GA is the score of correct pixels identified as being parks. As a result of the final algorithm, we obtain a set of white pixels belonging to the predicted class.

2.5. Multi-Layered Based-PCNN (MLB-PCNN)

The model proposed by our team is a complex combination of 12 operations, combining several algorithms in a specific sequence - as shown in Figure 1. In the beginning these actions are performed: the algorithm receives information from two different spectral images, it then processes them with the Non Binary PCNN algorithm; once this operation is done, it adds the results. The next step consists of applying a threshold on the matrix resulted from the previous step and then it passes the result to a Non Binary PCNN algorithm. The resulting matrix undergoes a thresholding step and then is fed into two different Non Binary PCNN algorithm . The results of these two algorithms are added and fed into a standard PCNN algorithm. The binary matrix that results from the standard PCNN is used to select the plausible pixels from three spectral images (two are the same as the initial images, and the third is selected automatically by the GA to maximize the performance). Using a sliding window the plausible pixels are introduced in a PCA algorithm that reduces the dimensions of the data. This data is classified using the SVM block, that decides if the data is representing a park or not.

3. DATASET DESCRIPTION

We will evaluate the results of our methods on a dataset of hyperspectral images extracted from the Sentinel-2 [13] satellites. The Sentinel-2 program offers images from a pair of satellites (Sentinel-2A and Sentinel-2B) consisting of 13 different spectral bands, with central wavelengths between 443 and 2190 nm, from the near visible and near-infrared (VNIR) and short-wave infrared (SWIR) at resolutions ranging from 10 meters to 60 meters. The declared mission of Sentinel-2 is to generate information relating to climate change, environmental policies, sustainable development, agriculture and risk management.

Band	Central wavelength	Resolution	Bandwidth
7	783	20	20
10	1375	60	20
11	1610	20	90

Table 1. Sentinel-2 used spectral bands.

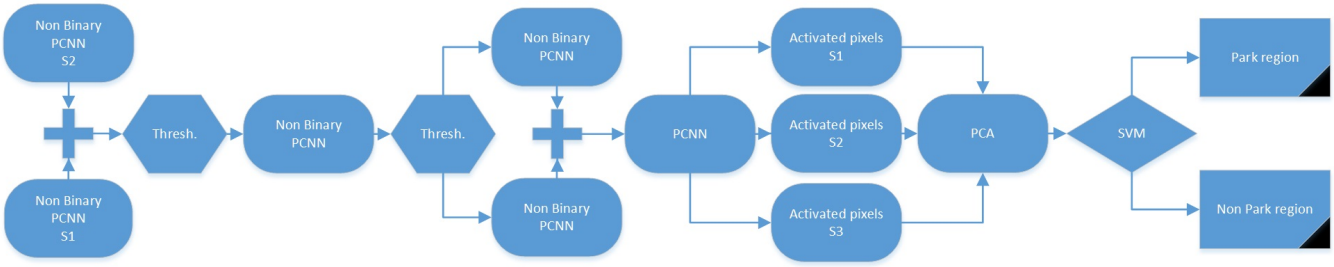

Fig. 1. Multi-Layered Based-PCNN (MLB-PCNN) algorithm framework.

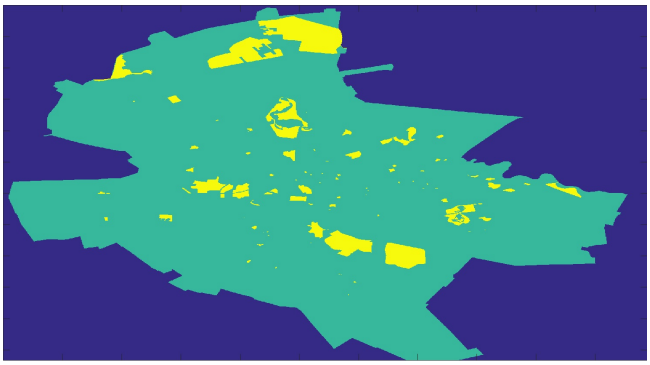

Fig. 2. Ground truth data. The area of Bucharest is shown in green, while the target parks are shown in yellow.

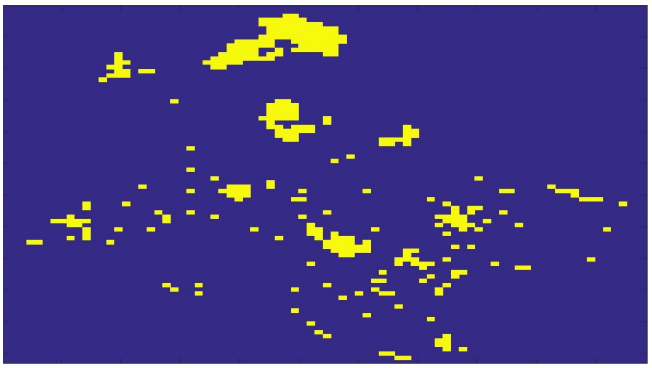

Fig. 3. Result: Precision: 0.4816, Recall: 0.7685. The blue pixels are the non-park pixels, while the detected parks are shown in yellow.

The images were taken from the *T35TMK* tile, from June 30th, 2017, a tile that contains the target city for our experiments, Bucharest. The resolutions of the tile images are: 1830×1830 for the spectral bands with 60 meter resolution, 5490×5490 for the 20 meter resolution and 10980×10980 for the 10 meter resolution.

Ground truth data, regarding the coordinates of the parks for the city of Bucharest, was collected from OpenStreetMap (OSM) [14] via the Overpass API. We collected all the target areas marked with the following tags: "leisure - park", "landuse - forest", "nature - heath", "tourism - theme_park", "boundary - national_park", "boundary - protected_area", "leisure - garden", "leisure - nature_reserve" and "natural - wood". This query returned 131 items, representing 6.69% of the total area of Bucharest, as shown in Figure 2.

4. EXPERIMENTAL RESULTS

In order to evaluate the performance of the proposed algorithm we decided to run a couple of tests. In the first test we used half of Bucharest's parks for training and the other half for testing. In the second test we decided to use 3/4 of the parks for training and the rest for tests. For comparison we tried to use several deep neural networks, including YOLO[15]. Unfortunately we could not obtain any significant results using these methods, most probably because the training set is extremely small. In consequence we decided to compare our results with a standard PCNN algorithm, whose parameters have been optimized with a GA and followed by the same sliding window-PCA-SVM algorithm for the identification of parks in Bucharest.

Algorithm	Precision	Recall
PCNN 1/2	0.3750	0.4098
PCNN 1/4	0.3341	0.5425
MLB-PCNN 1/2	0.5429	0.4005
MLB-PCNN 1/4	0.4816	0.7685

Table 2. Experimental results. Results are calculated at pixel level.

The metrics used for describing the performance of the algorithms, Precision and Recall, were calculated at pixel level, meaning $P = TP/(TP + FP)$ and $R = TP/(TP + FN)$, where TP is the number of true positive predicted pixels, FP is the number of false positive pixels and FN is the number of false negative pixels. Here we must mention that the GA has determined that the best spectral bands to be used are the 7, 10 and 11, as shown in Table 1, and the SVM kernel is

linear, which proves that the data is linearly separable. The results can be seen in Table 2. As seen in the results table, the proposed algorithm benefits considerably from an increase in the number of examples it receives for training. Therefore the best results were achieved when the training data consisted of 3/4 of the total number of parks, with a pixel level Recall value of 0.7685.

5. CONCLUSIONS AND FUTURE WORK

The proposed method has proven that it can identify 76.85% of the required pixels and that it can obtain adequate results from a very small training set (6.69% * 3/4 of the total number of pixels), representing a state of the art result when compared with other approaches. This method generated a useful tool for exploiting the publicly available data provided by various satellite systems (e.g. the Sentinel-2 program) in an urban ecological effort.

In the future we plan to test this algorithm by using one city for training and other ones for testing, and even chaining the number and the nature of the represented classes, by predicting other nearly indistinguishable areas.

6. ACKNOWLEDGMENTS

This work was supported by the Romanian Space Agency (ROSA), contract STAR-C3-160/2017 and Romanian UEFISCDI Agency under projects PN3-483/2017 and PN3-PED-147/2017.

7. REFERENCES

[1] Abdul Qayyum, Aamir Saeed Malik, Muhammad Naufal Bin muhammad Saad, and Mahboob Iqbal, "Segmentation of satellite imagery based on pulse-coupled neural network," in *Space Science and Communication (IconSpace), 2015 International Conference on*. IEEE, 2015, pp. 393–397.

[2] JS Deng, K Wang, YH Deng, and GJ Qi, "Pca-based land-use change detection and analysis using multitemporal and multisensor satellite data," *International Journal of Remote Sensing*, vol. 29, no. 16, pp. 4823–4838, 2008.

[3] Tengyun Hu, Jun Yang, Xuecao Li, and Peng Gong, "Mapping urban land use by using landsat images and open social data," *Remote Sensing*, vol. 8, no. 2, pp. 151, 2016.

[4] MA Gilabert, J González-Piqueras, FJ Garcıa-Haro, and J Meliá, "A generalized soil-adjusted vegetation index," *Remote Sensing of environment*, vol. 82, no. 2, pp. 303–310, 2002.

[5] Angela Kross, Heather McNairn, David Lapen, Mark Sunohara, and Catherine Champagne, "Assessment of rapideye vegetation indices for estimation of leaf area index and biomass in corn and soybean crops," *International Journal of Applied Earth Observation and Geoinformation*, vol. 34, pp. 235–248, 2015.

[6] Reinhard Eckhorn, Herbert J Reitboeck, Mt Arndt, and P Dicke, "Feature linking via synchronization among distributed assemblies: Simulations of results from cat visual cortex," *Neural computation*, vol. 2, no. 3, pp. 293–307, 1990.

[7] John L Johnson, "Pulse-coupled neural nets: translation, rotation, scale, distortion, and intensity signal invariance for images," *Applied Optics*, vol. 33, no. 26, pp. 6239–6253, 1994.

[8] Victor-Emil Neagoe, Adrian-Dumitru Ciotec, and Serban-Vasile Carata, "A new multispectral pixel change detection approach using pulse-coupled neural networks for change vector analysis," in *Geoscience and Remote Sensing Symposium (IGARSS), 2016 IEEE International*. IEEE, 2016, pp. 3386–3389.

[9] G Kuntimad and Heggere S Ranganath, "Perfect image segmentation using pulse coupled neural networks," *IEEE Transactions on Neural Networks*, vol. 10, no. 3, pp. 591–598, 1999.

[10] C Bishop, "Pattern recognition and machine learning (information science and statistics), 1st edn. 2006. corr. 2nd printing edn," *Springer, New York*, 2007.

[11] Corinna Cortes and Vladimir Vapnik, "Support vector machine," *Machine learning*, vol. 20, no. 3, pp. 273–297, 1995.

[12] Kim-Fung Man, Kit-Sang Tang, and Sam Kwong, "Genetic algorithms: concepts and applications [in engineering design]," *IEEE transactions on Industrial Electronics*, vol. 43, no. 5, pp. 519–534, 1996.

[13] P Martimor, Olivier Arino, Michael Berger, Roberto Biasutti, Bernardo Carnicero, Umberto Del Bello, Valérie Fernandez, Ferran Gascon, Pierluigi Silvestrin, François Spoto, et al., "Sentinel-2 optical high resolution mission for gmes operational services," in *Geoscience and Remote Sensing Symposium, 2007. IGARSS 2007. IEEE International*. IEEE, 2007, pp. 2677–2680.

[14] OpenStreetMap, "http://www.openstreetmap.org/," .

[15] Joseph Redmon, Santosh Divvala, Ross Girshick, and Ali Farhadi, "You only look once: Unified, real-time object detection," in *Proceedings of the IEEE Conference on Computer Vision and Pattern Recognition*, 2016, pp. 779–788.